Optical Focusing-based Adaptive Modulation for Optoacoustic Communication

Muntasir Mahmud, Md Shafiqul Islam, Mohamed Younis and Gary Carter
Department of Computer Science and Electrical Engineering,
University of Maryland Baltimore County
Baltimore, Maryland, USA
mmahmud1, mdislam1, younis, carter@umbc.edu

2021 30th Wireless and Optical Communications Conference (WOCC) | 978-1-6654-2772-2/21/$31.00 ©2021 IEEE | DOI: 10.1109/WOCC53213.2021.9603005

Abstract— Wireless communication from air to underwater is a longstanding challenge that can be addressed by the optoacoustic process. We can directly transmit data to underwater submerged nodes from the air with proper modulation technique by varying basic laser parameters, e.g., laser focusing angle from air to water. Laser-induced underwater plasma volume and shape are important because the duration and directivity of the generated acoustic pulses depend on these. Non-spherical shaped plasma generates anisotropic acoustic pressure; thus it is difficult to communicate from air to an unknown positioned underwater node. In this paper, we analyze how to control the shape of the plasma and propose an optical focusing-based adaptive modulation (OFAM) technique that enables transmission to underwater nodes even if the node's position is unknown. Bit error rates (BER) for different underwater node positions are analyzed, and the BER performance is compared with a lower pulse energy laser. Our results indicate that the performance is better if the underwater node position is in the direction of the laser beam, also when the laser focusing angle varies the most and a higher energy laser is used.

Keywords: Air-water communication, Optoacoustic, Optical focusing-based adaptive modulation, Bit error rate.

I. INTRODUCTION

Recent years have witnessed major advances in acoustic communication and underwater networking technologies, motivated by applications such as search and rescue, security surveillance, sea-based combat, marine biology, etc. The conventional architecture for an underwater network involves a surface (floating) node, e.g., a buoy, or a boat, that serves as a gateway for connecting the nodes to remote command and data collection centers. Such a gateway is equipped with dual transceivers: (1) an acoustic for reaching underwater nodes and (2) a radio for communication over air. However, the required presence of a gateway has some significant shortcomings, such as: (i) it could constitute a logistical constraint that complicates the deployment, particularly for emerging situations such as search and rescue, e.g., to find a crashed passenger airplane; (ii) it could expose the underwater network to security risk. For military and security-sensitive applications, the gateway node could be located, and consequently, the presence of underwater nodes could be uncovered; (iii) it could complicate the operation of mobile underwater networks by imposing the need for fine-grained coordination during motion.

Avoidance of gateway nodes requires the development of a cross-medium communication scheme. However, no single type of wireless signal can operate well across different mediums. High-frequency radio waves transmit data near light speed in the air but die very rapidly after entering the water. Low-frequency radio waves have less attenuation coefficient in water, yet it is challenging to build antennas that can radiate such long waves underwater. Visible light communication (VLC) can be effective for short to moderate underwater range, but visual light beams get quickly scattered and cannot support long-range communication [1]. Acoustics has been the prime choice for communication in the water medium [2]; however, an acoustic signal mostly attenuates when crossing the water surface. While electromagnetic induction could be a possible means, it is not practical as the antenna is very large and the range is very limited.

A viable option for tackling the air-water cross-medium communication challenge is to exploit the optoacoustic effect. Alexander Graham Bell was the first to discover the optoacoustic effect in 1881 [3]. He noticed that when high-intensity light impinges on a liquid medium like water, an acoustic signal is generated. The optoacoustic energy conversion process could be divided into two mechanisms, linear and nonlinear. In the linear case, the properties of the water medium do not change. On the other hand, a nonlinear optoacoustic mechanism changes the physical properties of the water medium; specifically, water becomes vapor which creates cavitation bubbles [4]. The nonlinear optoacoustic process is suitable for reaching underwater receivers far from the surface because it generates a better sound pressure level (SPL) than the linear counterpart. The simulation results in [4] have shown that the SPL for a linear optoacoustic process yields up to 140 dB re 1 μPa. Meanwhile, the SPL of a nonlinear optoacoustic effect is as high as 185.61 dB re μPa at 1 m, and over 210 dB re μPa at 1 m have been reported in [5] and [6], respectively.

Little attention has been paid so far to the development of the communication protocol stack for nonlinear optoacoustic. This paper tackles the first step to fill such a technical gap, by devising a suitable modulation scheme. Unlike communication links through radio, acoustics, and visual light, exploiting the optoacoustic effect, in essence, involves two distinct signal types, precisely, optical (laser beam) in the air and acoustic in the underwater. In other words, it is necessary to modulate the laser beam such that the resulting acoustic signals could be demodulated to retrieve the data correctly. Such a modulation challenge is unique and cannot be handled by traditional schemes. Hence the development of an unconventional modulation mechanism is indeed warranted. This paper first analyzes how to set the basic laser parameters to control the generated acoustic signal. Particularly we analyze the shape and size of the plasma that is induced by the laser and how it affects the strength of the resulting acoustic signal. We point out the relationship between the laser focus in the underwater and the shape and size of the plasma, and then propose a novel Optical Focusing-based Adaptive Modulation (OFAM) technique for optoacoustic communications. The main idea of OFAM is to dynamically adjust the lenses that concentrate the laser beam to control the focus spot size. To realize OFAM in practice, advanced designs of electronically controlled optical lenses could be leveraged [7]. The simulation results confirm the viability of our approach and characterize the bit error rate for different underwater node locations. To the best of our knowledge, OFAM is the first modulation technique based on optical focusing and the first for nonlinear optoacoustic links.

This paper is organized as follows. In section II, the laser-induced plasma shape and size control are analyzed. Section III provides a detailed description of our proposed modulation technique for nonlinear optoacoustic communications. Section IV analyses the performance and discusses the bit error rates for varying laser focus and pulse energy. Section V discusses the related work. The paper is concluded in Section VI.

II. Plasma Shape and Size Control

Laser-induced optical breakdown is a nonlinear absorption process that leads to plasma formation at the locations where the breakdown threshold irradiance is exceeded. This plasma formation is associated with breakdown shockwave, cavitation bubble expansion, and collapse; such bubble collapse introduces shock wave (or waves) emission. The breakdown threshold is related to the laser pulse duration. By reducing the pulse duration, the energy threshold for breakdown decreases, and the irradiance threshold increases. A. Vogel et al. [8] have studied the thresholds for different pulse durations and focusing angles. For a few nanosecond pulse durations, the irradiance threshold values are in the order of 10^{11} W/cm^2 and 10^{13} W/cm^2 for 100 femtosecond pulse duration in order to generate plasma in water [9]. Figure 1 shows the Gaussian laser beam focusing with a convex lens. Laser irradiance (I) can be measured by laser peak power divided by the focal spot area. Here, the peak power is calculated by dividing the laser pulse energy (E) by pulse duration (τ_L). Thus, the laser irradiance is,

$$I = \frac{E/\tau_L}{A_f} \tag{1}$$

Here, the focal spot area, $A_f = \pi\omega_0^2$, with spot radius:

$$\omega_0 = \frac{\lambda f M^2}{\pi\,(D/2)} \tag{2}$$

In Eq. (2) λ is the wavelength of the laser beam, f is the focal length of the lens, and D is the diameter of the laser beam. The beam propagation ratio is M^2, which indicates how close a laser is to a single-mode TEM00 beam and also defines how small a beam waist can be focused. Having M^2 equals to 1 implies the perfect Gaussian condition, and the focused spot is diffraction limited. Thus, the diffraction-limited focus spot radius is,

$$\omega_0 = \frac{2\lambda}{\pi}\cdot\frac{f}{D} \tag{3}$$

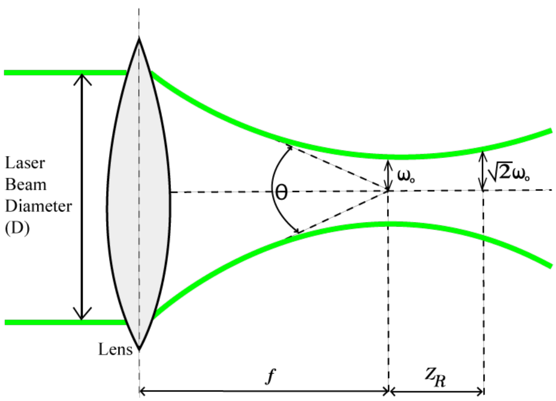

Figure 1: Gaussian laser beam focusing with a convex lens.

Based on Eq. (3), to decrease the focal spot area, a lens with a shorter focal length needs to be used, or the laser beam diameter has to be increased. Here, the ratio of focal length to beam diameter is known as *f*-number ($f/\# = \frac{f}{D}$). To create underwater plasma, high-intensity laser pulses need to be focused into a small spot so that the laser irradiance surpasses the breakdown threshold irradiance. Increasing the pulse energy or decreasing the *f*-number will boost the laser irradiance in the focused spot to generate the plasma, which is the source of the acoustic wave. In order to control the acoustic wave, we need to control the size and shape of the underwater plasma. The length of this generated plasma (z_{max}) reached at maximum irradiance for a laser pulse with Gaussian shape; the beam profile has been shown in [10] to be,

$$z_{max} = z_R\sqrt{\beta - 1} \tag{4}$$

where, the normalized laser pulse energy, $\beta = \frac{E}{E_{th}} = \frac{I}{I_{th}}$ and the Rayleigh range, $z_R = \frac{\pi\omega_0^2}{\lambda}$. By substituting the value of z_R in (4) we have,

$$z_{max} = \frac{\pi\omega_0^2}{\lambda}\sqrt{\beta - 1} \tag{5}$$

The dependency of maximum plasma length (z_{max}) on the focusing angle (θ) is given in [11] as,

$$z_{max} = \frac{\lambda}{\pi\tan^2\frac{\theta}{2}}\sqrt{\beta - 1} \tag{6}$$

In Eq. (5) and (6), the dependence of z_{max} on the laser pulse duration is implicit; determining z_{max} requires knowledge of the breakdown threshold E_{th} or I_{th} to calculate β for each laser pulse energy and duration. The calculated plasma length and experimentally measured data are almost identical for picosecond pulses but not as close for nanosecond pulses [11]. One reason can be the breakdown threshold which is influenced by plasma radiation; such breakdown threshold decreases during the nanosecond breakdown but remains approximately constant during the picosecond breakdown process [11]. Thus, the length of the nanosecond plasma grows further than predicted using Eq. (5) and (6), which assume a constant threshold. Another reason for getting longer plasma length from experiments is the optical aberration and diffraction-limited calculation. For example, if the diffraction-limited spot radius is half of the measured spot radius, then the corresponding Rayleigh range is four times greater, and the plasma length will increase accordingly. It is evident from Eq. (6) that the plasma will be more elongated for higher energy laser pulses. Also, z_{max} is dependent on the focusing angle and focal spot radius, which are inversely related; increasing the focusing angle will decrease the spot size, and thus the plasma length will decrease.

A shorter plasma length implies a more spherical shape; as the plasma length elongates, the shape becomes more cylindrical. An elongated plasma is considered a non-spherical acoustic source that generates anisotropic acoustic pressure. A spherical acoustic source can generate isotopic pressure in all directions, but with the elongation, the pressure becomes more anisotropic, and the peak pressure is in a direction that is perpendicular to the laser propagation [12]. For a narrowband 532 nm or 1064 nm laser source, the minimum pressure is in

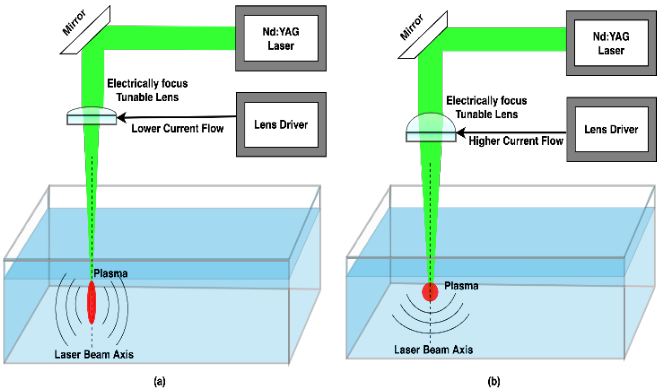

Figure 2: (a) Cylindrical (b) spherical shaped plasma generation in water using an electronically focus-tunable lens.

the direction of the laser beam, and the pressure direction changes from 0^0 to 90^0 along the laser beam axis [13]. The pressure difference in all directions can be decreased by making the shape of the plasma more spherical.

To control the acoustic pressure, we can vary the laser pulse energy or focusing angle. For a fixed *f*-number, increasing the pulse energy results in a more elongated acoustic source, and Energy Spectral Density (ESD) that is peaked at a lower frequency [13]. However, increasing the focusing angle will create continuous, more condensed single core plasma for fixed pulse energy, which will be more spherical in shape [14]. Thus, we can decrease the pressure difference between 0^0 to 90^0 by increasing the focusing angle where the pressure in the 0^0 direction grows but the pressure in the 90^0 direction diminishes. Figure 2 illustrates the change of focal length by varying the current flowing to an electrically tunable lens using a lens driver. A weak current flow leads to a shallow focus angle, thus creating cylindrical shaped plasma; meanwhile a higher current flow yields a larger focus angle, and thus creates spherical shaped plasma. Sinibaldi et al. [15] have captured the plasma sphericity as a function of laser pulse energy and focusing angle, where the plasma is more spherical for higher focusing angles, and sphericity index (ratio of plasma thickness to plasma length) is around 0.7-0.8 at threshold energy but limited to ≤ 0.4 at large energies, regardless of the focusing angle.

III. Optical Focusing-based Adaptive Modulation (OFAM) for Optoacoustic Communication

We are considering the laser-induced plasma as the antenna for the acoustic emission, where the shape of the antenna can be changed by varying the focusing angle of the laser. The idea is to dynamically control the focal length by using electrically focus-tunable lenses. These advanced lenses are driven by electrical current, and the focal length of the lens is a function of the electrical current [7]. The stronger the current is, the shorter the focal length becomes. Thus, the focusing angle of the lens can be increased. Y. Tagawa et al. [12] have measured the near field peak pressure of a laser-induced underwater shockwave generated by using 5x, 10x, and 20x objective lenses where the focusing angles of the lens are 1^0, $4^{0,}$ and 6^0, respectively. A 532 nm, 6 ns Nd:YAG laser was used, and the hydrophone was placed 0^0 and 90^0 directions from the laser beam axis. Figure 3 is regenerated from [12]. As shown in the figure, increasing the focusing angle increases the peak pressure at the 0^0 direction but decreases the peak pressure at 90^0 directions. From this observation, we can conclude that the plasma becomes more spherically-shaped with the increasing focusing angle, and the pressure difference between 0^0 and 90^0 directions has decreased. One exception is at the 90^0 direction for 2.6 mJ, where the peak pressure has increased in the 10x objective lenses more than the 5x counterpart.

Traditional OOK modulation by varying the focusing angle is not suitable for an underwater node with an unknown position. This is because the generated peak pressure is not the same in all directions, and varying the focusing angle does not change the peak pressure similarly in both the 0^0 and 90^0 directions. Hence, without knowing its position relative to the laser incident point on the surface, the underwater node cannot surely determine whether the received peak pressure value will increase or decrease if the focusing angle changes. To overcome this issue, we pursue a novel dynamic modulation technique that will enable effective air-water optoacoustic.

In our OFAM technique, the underwater node first receives fixed control bits to map the certain peak pressure values for a small focusing angle and a large focusing angle. Then the node calculates a threshold for demodulation by averaging the received peak pressure values. The received message data payload bits are demodulated by factoring in the amplitude of the received control bits, and comparing with the threshold. Thus, this modulation technique can work dynamically despite the unknown underwater node position. A pseudo-code summary of the steps for the OFAM modulation technique and bit error rate calculation is shown in Algorithm 1. The following explains the steps:

Step 1: First, the key parameters, specifically, the control bits (*Cbits*) and message data payload bits (*D*) need to be determined. *Cbits* should be a mix of alternative high and low bits that the underwater node is already aware of. For example, *Cbits* = [0 1 0 1] or *Cbits* = [1 0 1 0], etc. To describe all the steps of Algorithm 1, we will consider *Cbits* = [0 1]. We also assume that 5x and 20x lenses are used so that we can leverage Figure 3 in the explanation.

Step 2-8: These steps are for mapping *Cbits* with the generated peak pressure values in the receiver. For example, we can map the bit '0' and bit '1' as the peak pressure generated from a small focusing angle and a large focusing angle, respectively. After mapping, the values are saved in *Cbits_P*.

Step 9-11: In these steps, noise is added with *Cbits_P* and *D*; the new values are *rcv_Cbits* and *D_noise,* respectively. The mean of *rcv_Cbits* constitutes a threshold for demodulation.

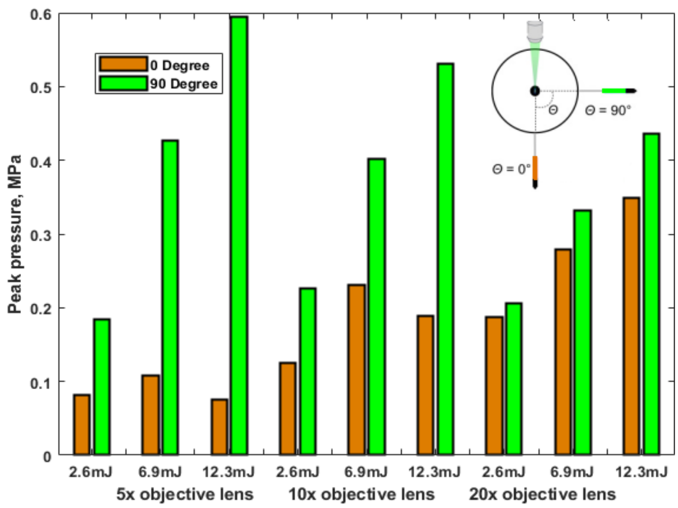

Figure 3: Peak pressure of a laser-induced underwater shockwave measured at 0^0 and 90^0 directions from the laser beam axis, regenerated from [12].

Step 12-17: The received message data payload bits are demodulated in two steps. At first, the peak pressure values of the even and odd bits of *rcv_Cbits* are compared. In this example, if the peak pressure for the 2nd bit of *rcv_Cbits* is higher than that of the 1st bit, then the values of *D_noise* which are greater than the *threshold* will be demodulated as a bit '1' and others as a bit '0'. In contrast, if the peak pressure of the 1st bit of *rcv_Cbits* exceeds that of the 2nd bit, the values of *D_noise* which are less than the *threshold,* will be demodulated as a bit '1' and the other as a bit '0'. The demodulated message data payloads are saved in *rcv_D.* If the peak pressure for the 2nd bit of *Cbits_P* is higher, it indicates, the underwater node is around the 0^0 direction; alternatively, if the peak pressure of the 1st bit of *Cbits_P* is higher, the underwater node is close to the 90^0 direction from the laser beam axis. Thus, OFAM can work accurately for different underwater node positions.

We note that the BER can be estimated as follows. First, the number of errors is calculated by the total number of mismatch values in *D* and *rcv_D.* Then, BER is determined by dividing the total number of errors by the total number of message data payload bits sent.

<u>Input:</u> Control Bits (Cbits), Message data payload (D),
<u>Output:</u> Bit Error Rate (BER)

---

1. *initialize: Cbits, D*
2. ***for*** *i=1:length of (Cbits)*
3.   ***if*** *Cbits (i) = 0*
4.   *Cbits_P (i) = peak pressure generated from small focusing angle*
5.   ***else***
6.   *Cbits_P (i) = peak pressure generated from large focusing angle*
7.   ***end if***
8. ***end for***
9. *rcv_Cbits = Cbits_P + noise*
10. *threshold = mean of the rcv_Cbits*
11. *D_noise = D + noise*
12. ***for*** *j= 1:length of (D)*
    if *sum of rcv_Cbits (odd bits) < sum of rcv_Cbits (even bits)*
13.   *rcv_D(j) = (D_noise > threshold)*
14.   ***else***
15.   *rcv_D(j) = (D_noise < threshold)*
16.   ***end if***
17. ***end for***

Algorithm 1. Pseudo code summary of the OFAM.

IV. Performance Analysis

Algorithm 1 has been implemented using MATLAB to analyze the BER of the proposed OFAM scheme. The data for simulation is taken from Figure 3. Here, the peak pressure data is available only in the 0^0 and 90^0 directions, and we calculated peak pressure at a 45^0 direction, using Figure 3 and [13]. The main objective of the validation is to identify angles for the laser focusing that generate less BER and consequently improve link robustness and bandwidth utilization. In addition, the simulation evaluates in what direction the underwater node should be in order to improve BER. We have used 8 control bits to calibrate the underwater receiver to calculate the threshold value and sent 10^5 randomly generated message data payload bits. We incorporated additive white Gaussian noise (AWGN) with the control bits and data bits and also calculated the theoretical BER using the *erfc* function.

Figures 4, 5, and 6 show the BER for fixed 12.3 mJ laser pulse energy. Figure 4 shows the BER vs. SNR using 5x and 20x objective lenses. As expected, the BER is decreasing with the increase of SNR. We can observe here that the lowest BER is in the 0^0 direction, and the highest is in the 45^0 direction. Figure 5 shows the results when 10x and 20x objective lenses are employed, where the BER is higher than that of Figure 4 in all the directions. Figure 6 plots the BER for 5x and 10x objective lenses. Here BER of 45^0 and 90^0 is the worst among the three considered configurations (i.e., higher than that of Figures 4 and 5) but BER for 0^0 is better than Figure 5.

Figures 7, 8, and 9 show the BER for the same objective lenses while using different laser pulse energy (6.9 mJ). Here, the 0^0 direction also has the lowest BER except for Figure 8, where the 90^0 direction yields better BER. When considering Figures 4-9 collectively, we can conclude that the best BER performance is achieved in Figure 4, where the focusing angle has varied the most. Moreover, the BER performance is better for 12.3 mJ than 6.9 mJ pulse energy. For both the laser pulse energy settings, the underwater node will have less BER if it is in the laser beam axis direction except the one case shown in Figure 8. The underwater node will experience poorer BER if it is in the 45^0 direction from the laser beam axis, as seen in all plots. The BER performance can be improved in the 45^0 direction if we employ 5x and 20x objective lenses and higher laser pulse energy, similar to Figure 4. Thus, the OFAM

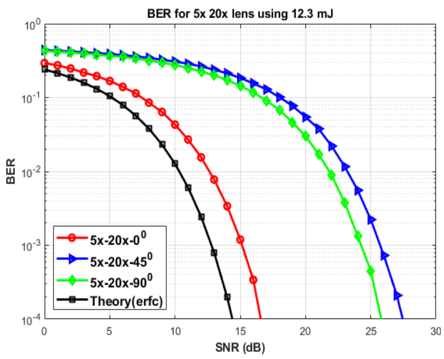

Figure 4: BER vs SNR using 5x and 20x objective lens for 12.3 mJ.

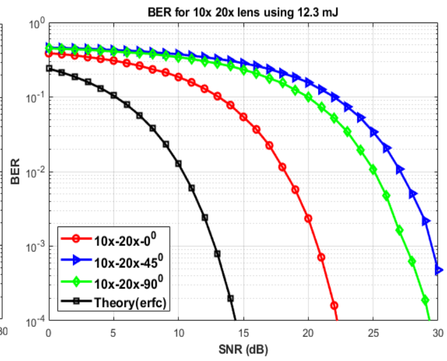

Figure 5: BER vs. SNR using 10x and 20x objective lenses for 12.3 mJ.

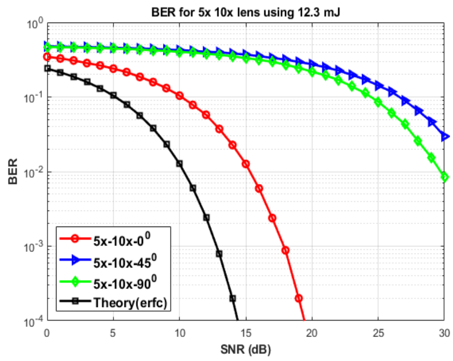

Figure 6: BER vs SNR using 5x and 10x objective lens for 12.3 mJ.

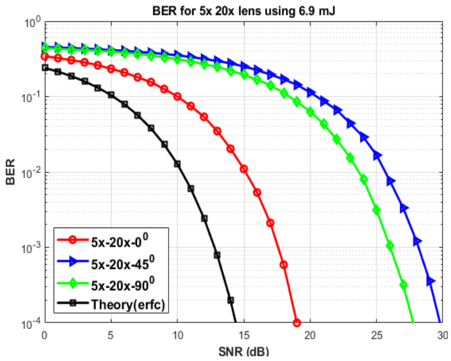

Figure 7: BER vs SNR using 5x and 20x objective lens for 6.9 mJ.

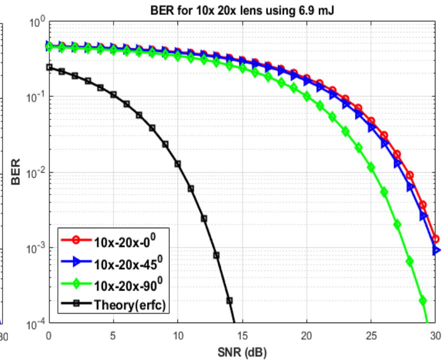

Figure 8: BER vs. SNR using 10x and 20x objective lenses for 6.9 mJ.

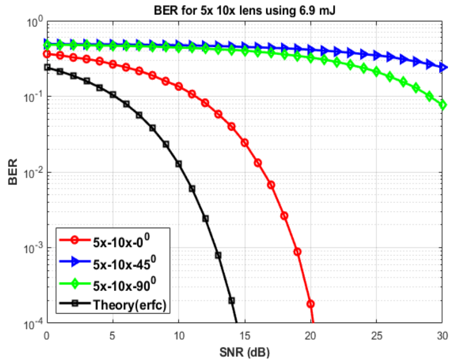

Figure 9: BER vs SNR using 5x and 10x objective lens for 6.9 mJ.

modulation technique performs better when a higher pulse energy laser is used and modulated with large focusing angle variations.

V. Related Work

Communication from air to underwater has attracted growing attention in recent years. A low frequency and low bit-rate MI communication system is designed by Sojdehei et al. [16] and tested from air to shallow water. Visual light has been considered as a prime choice, given its ability to penetrate the water surface. Islam and Younis [17] have developed an adaptive differential pulse position modulation scheme to enable energy-efficient communication from an airborne base station to underwater nodes using VLC. Laser beams have also been pursued; in a recent work [18], an overlapping pulse position modulation (OPPM) scheme has been applied. However, regardless of whether MI, visual light or laser are used, the modulation and demodulation are based on the same signal. Optoacoustic communication includes two different signal types, i.e., optical in air and acoustic in water. Thus, it is challenging to modulate the laser beam and retrieve accurate data by demodulating the generated acoustic signal in water. Very few studies have been dedicated to devising modulation techniques for optoacoustic communication. Blackmon et al. [5] have varied the laser pulse repetition rate to demonstrate a method for controlling the generated underwater acoustic signal spectrum. However, for the high repetition rate of the laser, after a few acoustic transients, further acoustic signal generation is precluded because of vapor cloud buildup in the vicinity of the focus area.

VI. Conclusions

The optoacoustic effect refers to the energy transfer from optical to acoustic when a high-power laser beam is directed to a water surface. Exploiting the optoacoustic effect to establish a communication link across the air-water interface can be beneficial in various application scenarios. This paper has presented OFAM, a novel modulation technique for optoacoustic communication. The size and shape of the underwater generated plasma can be controlled by varying basic laser parameters. Using an electrically tunable lens we can dynamically adjust the focusing angle for applying OFAM. The BER performance of OFAM is evaluated for different positions of the underwater node. The simulation results have confirmed that OFAM yields better performance when the focusing angle is varied the most using a higher pulse energy laser, and the underwater node position is in the direction of the laser beam.

Acknowledgement: This work is supported in part by the National Science Foundation, USA, contract #0000010465.

References

[1] M. S. Islam and M. F. Younis, "Analyzing visible light communication through air–water interface," *IEEE Access*, 7, pp. 123830-123845, 2019.

[2] D. Pompili and I. F. Akyildiz, "Overview of Networking Protocols for Underwater Wireless Communications," *IEEE Communications Magazine*, Vol. 47, No. 1, pp. 97 – 102, Feb. 2009.

[3] A. G. Bell, "Upon the production of sound by radiant energy," Philos. Magazine. 5(11), 510, 1881.

[4] Blackmon, F, Estes, L., and Fain, G., "Linear opto-acoustic underwater communication," *Applied Optics*, Vol. 44, No. 18, June, 2005

[5] Blackmon, F. and Antonelli, A., "Experimental demonstration of multiple pulse nonlinear opto-acoustic signal generation and control," *Applied Optics, Vol. 44, No. 1*, Jan. 2005, 103-112.

[6] T. G. Jones, M. Hornstein, A. Ting, D. Gordon and Z. Wilkes, "Characterization of underwater laser acoustic source for navy applications," *Proc. of the IEEE International Conference on Plasma Science* - Abstracts, San Diego, CA, 2009.

[7] "Focus Tunable Lenses." Optotune. Accessed October 30, 2020. [Online]. Available: https://www.optotune.com/focus-tunable-lenses.

[8] Vogel, A., Noack, J., H¨uttmann, G., Paltauf, G.: "Mechanism of femtosecond laser nanosurgery of cells and tissues," *Appl. Phys. B* 81, 1015–1047, 2005.

[9] Lauterborn W., Vogel A. (2013) "Shock Wave Emission by Laser Generated Bubbles," In: Delale C. (eds) Bubble Dynamics and Shock Waves. Shock Wave Science and Technology Reference Library, vol 8.

[10] F. Docchio, P. Regondi, M. R. C. Capon, and J. Mellerio, "Study of the temporal and spatial dynamics of plasmas induced in liquids by nanosecond Nd :YAG laser pulses 1—Analysis of the plasma starting times," *Appl. Opt.*, vol. 27, pp. 3661–3668, 1988.

[11] A. Vogel, K. Nahen, D. Theisen and J. Noack, "Plasma formation in water by picosecond and nanosecond Nd:YAG laser pulses. I. Optical breakdown at threshold and superthreshold irradiance," *IEEE Journal of Selected Topics in Quantum Electronics*, vol. 2, no. 4, pp. 847-860, 1996.

[12] Y. Tagawa, S. Yamamoto, K. Hayasaka, and M. Kameda, "On pressure impulse of a laser-induced underwater shockwave," *J. Fluid Mech*, Col. 808, No. 5, 2016.

[13] T.G. Jones, M. Helle, A. Ting, and M. Nicholas, "Tailoring Underwater Laser Acoustic Pulses", *NRL REVIEW, acoustics*, pp. 142-143, 2012.

[14] Tian, Y.; Wang, L.; Xue, B.; Chen, Q.; Li, Y., "Laser focusing geometry effects on laser-induced plasma and laser-induced breakdown spectroscopy in bulk water," *Journal of Analytical Atomic Spectrometry* 2019, 34(1), 118-126.

[15] Sinibaldi, G., et al., "Laser induced cavitation: plasma generation and breakdown shockwave," *Phys. Fluids,* 31(10), 2019, 103302.

[16] J. J. Sojdehei, P. N. Wrathall, and D. F. Dinn, "Magneto-inductive (MI) communications," in *Proc. MTS/IEEE Oceans*, Honolulu, HI, USA, Nov. 2001, pp. 513–519.

[17] M. S. Islam and M. Younis, "An Adaptive DPPM for Efficient and Robust Visible Light Communication Across the Air-Water Interface," *29th Wireless and Optical Comm. Conf. (WOCC)*, Newark, NJ, USA, 2020.

[18] Carver, Charles J., Tian Zhao, H. Zhang, K. Odame, Alberto Quattrini Li and Xia Zhou. "AmphiLight: Direct Air-Water Communication with Laser Light." *Proc, of the 17th USENIX Symp. on Networked Systems Design and Implementation (NSDI)*, Santa Clara, CA, February 2020.